

The SARS-Coronavirus PLnc domain of nsp3 as a replication/transcription scaffolding protein

Isabelle Imbert^a, Eric J. Snijder^b, Maria Dimitrova^c, Jean-Claude Guillemot^a,
Patrick Lécine^{d,e,f,1}, Bruno Canard^{a,*,1}

^a Centre National de la Recherche Scientifique and Universités d'Aix-Marseille I et II, UMR 6098, Architecture et Fonction des Macromolécules Biologiques, Ecole Supérieure d'Ingénieurs de Luminy-Case 925, 163 Avenue de Luminy, 13288 Marseille Cedex 9, France

^b Molecular Virology Laboratory, Department of Medical Microbiology, Center of Infectious Diseases, Leiden University Medical Center, LUMC P4-26, P.O. Box 9600, 2300 RC Leiden, The Netherlands

^c INSERM U748, Institut de Virologie, 3 rue Koeberlé, 67000 Strasbourg, France

^d Inserm, U599, Centre de Recherches en Cancérologie de Marseille, Marseille F-13009, France

^e Institut Paoli-Calmettes, Marseille F-13009, France

^f Univ Méditerranée, F-13007 Marseille, France

Received 18 July 2007; received in revised form 12 November 2007; accepted 21 November 2007

Available online 5 February 2008

Abstract

Many genetic and mechanistic features distinguish the coronavirus replication machinery from that encoded by most other RNA viruses. The coronavirus replication/transcription complex is an assembly of viral and, most probably, cellular proteins that mediate the synthesis of both the unusually large (~30 kb) RNA genome and an extensive set of subgenomic mRNAs. The viral components of the complex are encoded by the giant replicase gene, which is expressed in the form of two polyproteins (pp1a and pp1ab) that are processed into 16 cleavage products (nonstructural proteins 1–16). Using the combination of yeast two-hybrid screening and GST pull-down assays, we have now analyzed all potential interactions between SARS-Coronavirus nonstructural proteins, which may contribute to the structure and/or function of the viral replication/transcription complex. We demonstrate the existence of a complex network of interactions involving all 16 nonstructural proteins. Our results both confirmed previously described associations and identified novel heterodimerizations. The interaction map thus provides a sum of the interactions that may occur at some point during coronavirus RNA synthesis and provides a framework for future research.

© 2007 Elsevier B.V. All rights reserved.

Keywords: Coronavirus; SARS-CoV; Replication; Protein interactions

1. Introduction

The family *Coronaviridae* includes the genera *Coronavirus* and *Torovirus* that, together with the more distantly related *Arteriviridae* and *Roniviridae* families, form the order *Nidovirales* (for reviews see Gorbalenya et al., 2006). In 2003, a novel coronavirus was identified as the etiological agent of the Severe Acute Respiratory Syndrome (SARS; Drosten et al., 2003; Ksiazek et al., 2003; Peiris et al., 2003) and is now known as the SARS-Coronavirus (SARS-CoV).

Coronaviruses are enveloped viruses with large positive-sense single-stranded RNA genomes ranging from 27 to 32 kb, the largest among the known RNA viruses. Like other nidoviruses, coronaviruses genomes are polycistronic with about two thirds being occupied by two large open reading frames (ORFs 1a and 1b) that specify the viral nonstructural proteins (nsps) or “replicase”. The coronavirus genome is expressed using a variety of regulatory mechanisms, including the synthesis and proteolytic processing of replicase polyproteins and the generation of an extensive nested set of subgenomic (sg) mRNAs to express structural and accessory proteins from the 3′-proximal part of the genome (for recent reviews, see Pasternak et al., 2006; Sawicki et al., 2007). Genome expression starts with the translation of replicase ORFs 1a and 1b, with expression of the latter involving a –1 ribosomal frameshift (Brierley et al., 1989;

* Corresponding author. Tel.: +33 491 82 86 44; fax: +33 491 82 86 46.

E-mail address: Bruno.Canard@afmb.univ-mrs.fr (B. Canard).

¹ These authors contributed equally to this work.

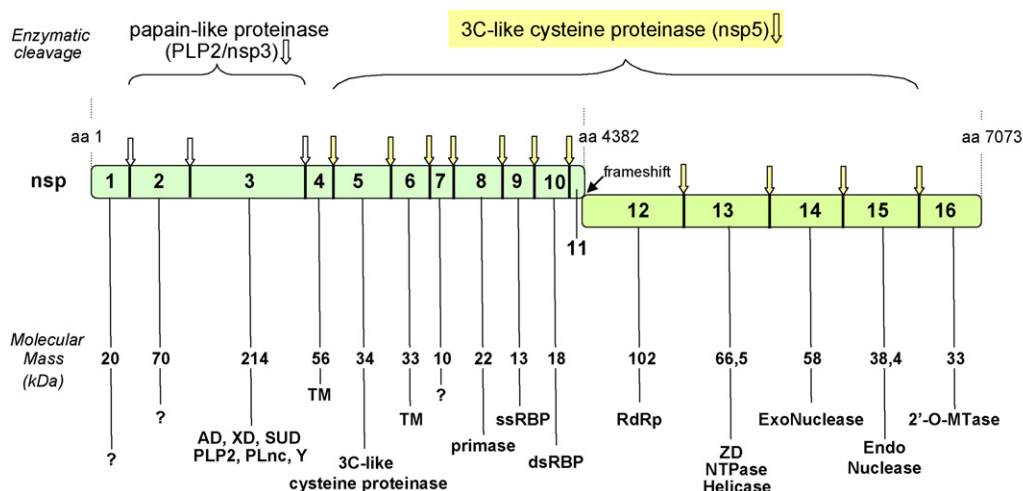


Fig. 1. SARS-CoV replicase organization. Cleavage products and their nomenclature, and (predicted) protein functions are depicted. Abbreviations: nsp, nonstructural protein; AD, acidic domain; XD, X domain; SUD, SARS-CoV unique domain; PLP2, papain-like proteinase; PLnc, papain-like noncanonical; Y, nsp3-Y domain; TM, transmembrane domain; ssRBP, single-strand RNA binding protein; dsRBP, double-strand RNA binding protein; RdRp, RNA-dependent RNA-polymerase; ZD, zinc-binding domain; 2'-O-MTase, 2'-O-methyltransferase; ?, unknown function.

Brierley and Dos Ramos, 2006) occurring with an estimated efficiency of 20–40%. In the case of SARS-CoV, pp1a and pp1ab are 4382 and 7073 amino acids long, respectively (Marra et al., 2003; Rota et al., 2003; Snijder et al., 2003; Thiel et al., 2003). These precursors are cleaved co- and post-translationally by two viral proteases, a papain-like protease (PLP2) residing in nsp3 and the 3C-like protease (3CLpro; nsp5), to produce the mature replicase subunits nsp1 to nsp16 (Fig. 1). Most of these subunits are believed to associate with a poorly characterized membrane-bound complex (Bost et al., 2001; Gosert et al., 2002; Shi et al., 1999; Snijder et al., 2006; van der Meer et al., 1999) that mediates the synthesis of genome RNA (replication) and sg mRNAs (transcription). The sg mRNAs are produced by a unique mechanism involving discontinuous negative-strand RNA synthesis to produce subgenome-length templates for sg mRNA synthesis (Sawicki and Sawicki, 1995; reviewed in Pasternak et al., 2006; Sawicki et al., 2007).

Knowledge related to the functions and interactions of coronavirus nsps has remained limited thus far. nsp1 and nsp2 are rather variable in sequence, and possibly subgroup-specific replicase subunits (Snijder et al., 2003; Ziebuhr et al., 2001). SARS-CoV nsp1 (20 kDa) was implicated in suppression of cellular gene expression by promoting host cell mRNA degradation (Kamitani et al., 2006) and in chemokine dysregulation (Law et al., 2007). SARS-CoV nsp2 (70 kDa) is dispensable for replication in cell culture, but its deletion attenuates viral replication (Graham et al., 2005). SARS-CoV nsp3 is a large multidomain protein of 1922 amino acids (Snijder et al., 2003; Thiel et al., 2003) that is thought to contain at least seven domains: (1) an N-terminal Glu-rich acidic domain (AD); (2) an X domain (XD) with poly(ADP-ribose) binding properties (Egloff et al., 2006; Saikatendu et al., 2005); (3) the SUD domain (for SARS-CoV Unique Domain, an insertion not found in any other coronavirus thus far) with a specific affinity for oligo(G)-strings (Tan et al., *in press*); (4) a papain-like protease (PLP2), recently shown to exhibit deubiquitinating activity (Barretto et al., 2005; Harcourt

et al., 2004; Lindner et al., 2005; Ratia et al., 2006); (5) an unknown domain possibly extending the papain-like protease domain, termed PLnc for Papain-Like noncanonical (see below); (6) a transmembrane domain (Kanjanahaluethai et al., 2007) corresponding to the N-terminal of the Y domain; and (7) the remainder of the Y domain, the abbreviation “Y domain” will be used for this part in this study. The multi-spanning transmembrane domains in nsp3, nsp4 and nsp6 are presumed to serve as a scaffold for the assembly of the membrane-associated replication/transcription complex (RTC). nsp5 (34 kDa) is a 3C-like cysteine protease (3CLpro), also known as “main protease” (M^{pro}) (Anand et al., 2003; Gorbalenya et al., 1989), cleaving the replicase polyproteins at 11 conserved sites containing a canonical Leu-Gln (Ser, Ala, Gly) signature. nsp8 protein (22 kDa) was recently postulated to be a processivity factor associated with the viral RNA-dependent RNA polymerase (RdRp) in nsp12. Indeed, the crystal structure of a hexadecameric nsp7–nsp8 complex provided a first glimpse of the sophisticated architecture of the coronavirus replication and transcription machinery (Zhai et al., 2005). The properties of the central channel of this complex suggest that it may encircle double-stranded RNA. This hypothesis was strengthened by the finding that nsp8 displays primase activity in an *in vitro* assay (Imbert et al., 2006) and might thus catalyse the synthesis of RNA primers for the primer-dependent RdRp. nsp9 (13 kDa) is a ssRNA-binding protein (Egloff et al., 2004; Sutton et al., 2004) postulated to stabilise and protect nascent and template RNA strands during replication and/or transcription. Much like nsp8 and nsp9, nsp10 (18 kDa) is also a nucleic acid-binding protein with two zinc fingers (Joseph et al., 2006; Matthes et al., 2006). The phenotype of a temperature-sensitive nsp10 mutant (Q65E) of the coronavirus mouse hepatitis virus (MHV) implicated nsp10 in minus-strand RNA synthesis (Sawicki et al., 2005; Siddell et al., 2001). The C-terminal part of nsp12 (102 kDa) contains the poorly characterized RdRp domain that is significantly divergent from both cellular and viral polymerases.

Table 1
SARS-CoV replicase subunits and domains used in this study

SARS-CoV nsp/domain	Genome position ^a of domains used in this study	Position in pp1a/pp1ab of domains used in this study
nsp1	nt 268–801	1Met-Gly180
nsp2	nt 802–2718	181Ala-Gly818
nsp3-AD	nt 2719–3294	819Ala-Leu1010
nsp3-XD	nt 3277–3786	1005Gln-Pro1174
nsp3-SUD	nt 3841–4890	1193Glu-Val1542
nsp3-PLP2	nt 4891–5817	1543Lys-Ser2025
nsp3-PLnc	nt 5818–6975	1852Thr-Pro2237
nsp3-Y	nt 7378–8484	2372Lys-Gly2739
nsp5	nt 9985–10902	3241Ser-Gln3546
nsp6	nt 10903–11772	3547Gly-Gln3836
nsp7	nt 11773–12021	3837Ser-Gln3919
nsp8	nt 12022–12615	3920Ala-Gln4117
nsp9	nt 12616–12954	4118Asn-Gln4230
nsp10	nt 12955–13371	4231Ala-Gln4369
nsp12	nt 13398–16166	4370Ser-Gln5301
nsp13	nt 16167–17969	5302Ala-Gln5902
nsp14	nt 17970–19550	5903Ala-Gln6429
nsp15	nt 19551–20588	6430Ser-Gln6775
nsp16	nt 20589–21485	6776Ala-Asn7073

^a All nucleotide numbers given refer to the SARS-CoV genome sequence (strain Frankfurt-1, GenBank accession number AY291315).

Only one study reported polymerase activity of a purified coronavirus RdRp (Cheng et al., 2005). nsp13 (67 kDa) comprises a C-terminal helicase domain with a 5′–3′ directionality and an N-terminal zinc-binding domain (Ivanov et al., 2004b; Seybert et al., 2000, 2005). Finally, nsp14 (58 kDa), nsp15 (38 kDa) and nsp16 (33 kDa) contain exoribonuclease (Minskaia et al., 2006), endoribonuclease (Bhardwaj et al., 2006; Ivanov et al., 2004a) and predicted 2′-O-ribose methyl transferase activities (von Grothuss et al., 2003), respectively, which are all essential for efficient coronavirus RNA synthesis (Almazan et al., 2006). In addition, as illustrated above, coronavirus replicases have evolved to include a number of nonessential functions that may provide a selective advantage in specific host cells only.

Most of the 16 coronavirus nsps are known or thought to be part of the RTC, which is formed following genome translation and replicase polyprotein processing. As for many plus-strand RNA viruses (Mackenzie, 2005; Salonen et al., 2004; Snijder et al., 2006), it has been demonstrated that nidovirus RNA synthesis is associated with cytoplasmic membranes, in this case double-membrane structures that likely originate from the endoplasmic reticulum. Obvious benefits of complex formation are the possibility to couple functions residing in different subunits and the sequestration of viral components. The complex and sophisticated coronavirus replication/transcription strategy suggests that the composition of the complex may change during the life cycle of the virus or that – alternatively – partially different complexes dedicated to, e.g. either replication or transcription may co-exist, probably relying on the same central RNA synthesizing catalytic subunit, the nsp12-RdRp.

The network of interactions within the SARS-CoV RTC has only begun to emerge. Dual-labelling studies in SARS-CoV-infected cells have confirmed the colocalization of a variety of replicase subunits (Harcourt et al., 2004; Ivanov et al., 2004a; Prentice et al., 2004; Snijder et al., 2006) and newly synthesized viral RNA (Harcourt et al., 2004). Chemical cross-

linking experiments demonstrated that SARS-CoV nsp10 could be cross-linked to nsp9 (Su et al., 2006), which in turn interacts with nsp8 (Sutton et al., 2004). Very recently, a SARS-CoV genome-wide analysis for intraviral protein–protein interactions was performed (von Brunn et al., 2007). Interactions were tested by yeast two-hybrid system and subsequently confirmed by co-immunoprecipitation experiments in mammalian cells. nsp2 and nsp8 showed a rather large number of interactions. In this study, the nsp3 protein was subdivided into 2 fragments by cutting to the SUD domain.

Coronavirus nsp12-RdRp is believed to play a central role in both replication and transcription. Here, we investigated interactions between all possible combinations of SARS-CoV nsps, including the nsp12-RdRp, which are potentially involved in the assembly and/or function of the RTC. The experiments were performed with *in vitro* translated nsps, as well as *ex vivo*, in *Saccharomyces cerevisiae* expressing these nsps in the context of a two-hybrid system. We observed a complex network of interactions involving all 16 nsps, confirming previously documented associations and identifying numerous novel heterodimerization events, and thus providing a framework for future research.

2. Materials and methods

2.1. Virus and sequence

The Frankfurt-1 isolate of SARS-CoV (GenBank accession number AY291315; Thiel et al., 2003) was amplified in Vero-E6 cells and used in this study for the production of the expression vectors.

2.2. Yeast two-hybrid matrix experiment

All protocols used for the yeast two-hybrid system were described previously (Walhout and Vidal, 2001). MaV103 and

MaV203 yeast strains (leu2-3112, tryp-901, his3 Δ 200, ade2-1, gal4A, gal80A, SPAL10::URA3, GAL1::lacZ, GAL1::HIS3-@LYS2, can1R, cyh2R), which are MATa and MATalpha, respectively, were used for the yeast two-hybrid matrix. RT-PCR products encoding different SARS-CoV proteins/domains, i.e. nsp1, nsp2, six nsp3 subdomains (AD, XD, SUD, PLP2, PLnc, and Y), nsp5 to nsp10, and nsp12 to nsp16 were first cloned into pDONR201 using the Gateway system (Invitrogen). All constructs were verified by sequence analysis. The boundaries of the domains used are detailed in Table 1. Using the Gateway system, each cDNA was subcloned into pAD and pDB vectors, which were used to transform MaV203 and MaV103 cells, respectively. Diploid cells were generated by mating MaV103 expressing genes fused to the DNA-binding domain (DB-ORF) and MaV203 expressing genes fused to the activation domain (AD-ORF). Selection was performed using selective complete (SC) medium lacking tryptophane and leucine. Patches representing potential interaction pairs were then examined for two-hybrid phenotypes by replica-plating onto selective plates, i.e. YPD (yeast extract, peptone, D-glucose) medium plate with a nitrocellulose filter on to perform the β -galactosidase filter lift assay, as well as on SC-Leu-Trp-His + 25 mM 3-AT and SC-Leu-Trp-Ura plates to assess the three two-hybrid phenotypes (β -galactosidase, His and Ura) (Walhout and Vidal, 2001). The matrix experiment was carried out three times, using clones derived from three different plasmid transformation and mating experiments.

2.3. Expression vectors

For GST fusion protein expression vectors, BamHI/EcoRI restriction fragments encoding the SARS-CoV PLnc domain, nsp8 and nsp9, and a BamHI restriction fragment encoding nsp12 were inserted in-frame into pGEX-4T-2 (GE Healthcare), to generate GST-PLnc, GST-nsp8, GST-nsp9 and GST-nsp12, respectively. GST-p55, encoding the HIV-1 Gag precursor, was constructed as described in Douaisi et al. (2004). To create SARS-CoV protein expression vectors, EcoRI/KpnI restriction fragments encoding nsp1, XD, SUD, PLP2, PLnc, Y, nsp5, nsp6, nsp7, nsp10, nsp16, EcoRI/XbaI restriction fragments encoding nsp2, nsp8, nsp9, AD, a XbaI/NotI restriction fragment encoding nsp12, and KpnI/NotI restriction fragments encoding nsp13, nsp14, nsp15 were cloned into pTNT (Promega). All constructs were sequenced, and the proteins expressed from these plasmids did not carry any foreign tags, except an additional N-terminal Met residue.

2.4. Protein expression in *E. coli* and purification

The GST-PLnc (69 kDa), GST-nsp8 (48 kDa), GST-nsp9 (38.8 kDa), GST-nsp12 (132 kDa) and GST-p55 (80 kDa) fusion proteins were expressed in *E. coli* strain C41(DE3) (Avidis SA, France), which contained the pLysS plasmid (Novagen). Bacterial cultures were grown at 37 °C in LB medium supplemented with ampicillin (100 μ g ml⁻¹) and chloramphenicol (17 μ g ml⁻¹) until the OD₆₀₀ reached 0.5. Protein expression was induced by adding 500 μ M isopropyl 1-thio-

β -D-galactopyranoside (IPTG) and cells were incubated for 4 h at 37 °C. In the case of GST-PLnc and GST-nsp12 expression, however, induction was performed with 100 μ M of IPTG and cells were incubated for 17 h at 17 °C. Cell pellets were resuspended in PBS supplemented with 0.25 mg ml⁻¹, of lysozyme, 0.1 mg ml⁻¹ DNase, 10 μ g ml⁻¹ RNaseA, 1 mM phenylmethylsulphonylfluoride (PMSF), protease inhibitor cocktail (Sigma), and 1% Triton X-100. The suspensions were sonicated and centrifuged at 25,000 \times g for 30 min, after which 500 μ l of a 50% slurry of glutathione-sepharose 4B beads (GE Healthcare) was added to the clarified supernatants. The beads were allowed to bind proteins for 1 h, washed three times with PBS, and finally resuspended in 500 μ l of PBS.

2.5. GST pull-down assays

RNAs specifying SARS-CoV nsp1, nsp2, nsp3 domains (AD, XD, SUD, PLP2, PLnc, Y), nsp5 to nsp10, and nsp12 to nsp16 were *in vitro* transcribed from the T7 promoter present in the pTNT expression vector. Transcripts were *in vitro* translated in the presence of [³⁵S]methionine using the TNT T7 coupled reticulocyte lysate system (Promega) according to the manufacturer's instructions. *In vitro* binding analyses were performed as described previously (Dimitrova et al., 2003). Each interaction was independently tested three times.

2.6. Western blot analysis

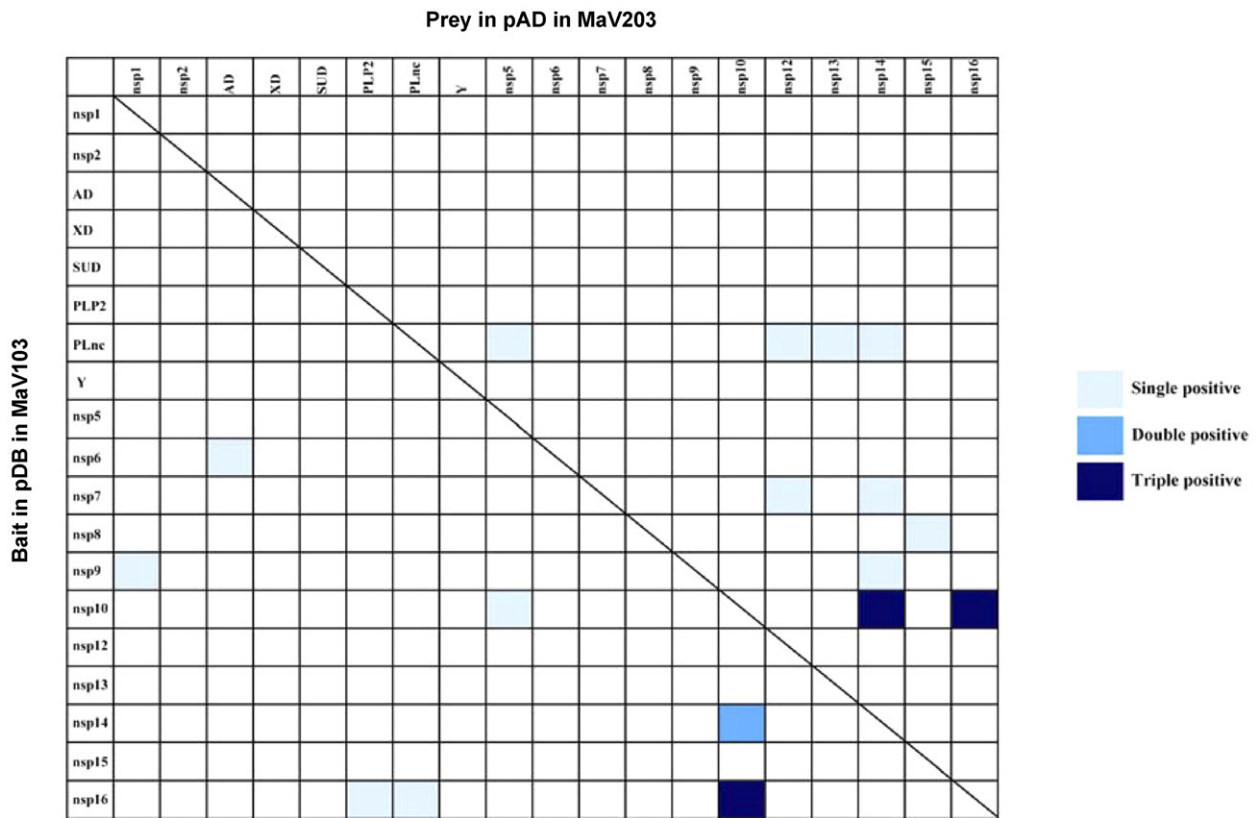
Protein samples were resolved by SDS-PAGE, transblotted onto Hybond-P membranes (GE Healthcare) and probed with an anti-GST antibody that was kindly provided by Dr. Teillaud (INSERM Unité 255, Paris, France).

3. Results and discussion

3.1. Yeast two-hybrid screening matrix for SARS-CoV nsps

The RTCs of mammalian positive-stranded RNA viruses, including coronaviruses, are commonly associated with intracellular membranes (Prentice et al., 2004; Snijder et al., 2006) and consist of multiple virus-encoded protein subunits as well as host proteins. To further characterize the molecular interactions between SARS-CoV RTC subunits, we performed a yeast two-hybrid matrix screen with all nsps encoded by this virus. An interaction was considered valid when it reproducibly produced a positive result for one or more of the three different yeast phenotypes tested (Fig. 2a). Subsequently, as a general strategy, GST pull-down assays were used to confirm interactions (see below). Because of the large size of the membrane-associated nsp3 (213 kDa), six nsp3 subdomains were defined (Table 1). The general bioinformatics approach that led to the design of nsp3 domains was described previously (Ferron et al., 2005). Briefly, we performed a BLAST search against the VaZyMoIO database with the full sequence corresponding to nsp3. The protein is predicted to be organized in 6 modules that are the F197 (AD) domain structurally confirmed by crystallography (Serrano et al., 2007), the F200 (XD) domain structurally confirmed by crystal-

(a)



(b)

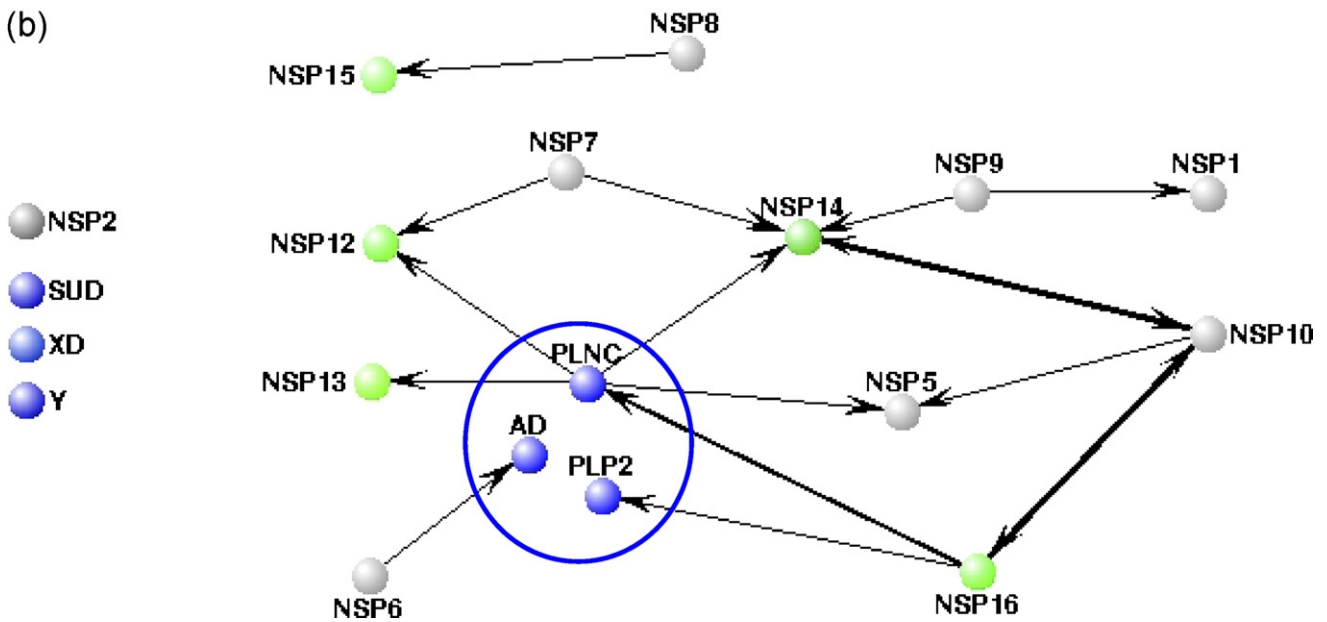


Fig. 2. (a) Analysis of SARS-CoV nonstructural protein interactions by Y2H matrix screen. Y2H matrix screen was performed by mating *S. cerevisiae* strains MaV203 and MaV103 containing prey and bait vectors with the respective SARS-CoV nsps on selective media. All nsps were tested against each other. Positive interactions in yeast are represented by squares with light blue, corresponding to single positive phenotype, azure blue corresponding to double positive phenotypes and dark blue corresponding to triple positive phenotypes. (b) Schematic representation of the outcome of the yeast two-hybrid matrix screen in which each SARS-CoV nsp was tested against all others. In view of its size, nsp3 (blue circle) was divided into a number of subdomains (see text) for the purpose of this experiment. Arrows indicate the interaction, from bait to prey. Thick arrows represent strong interactions (a positive result for all three phenotypes tested) and thin arrows indicate weaker interactions (one or two positive results). Nodes in blue and green represent nsp3 domains and ORF1b-encoded proteins, respectively. No interaction partners were identified for the proteins represented on the left side of the figure.

lography (Egloff et al., 2006), the F209 (SUD), the F203 (PLP2) domain also structurally confirmed by crystallography (Ratia et al., 2006), the F250 (PLnc) (Tan et al., in press), and a hydrophobic domain followed by the F202 (Y domain). The hydrophobic cluster analysis of module F250 (PLnc domain) can be interpreted as a single and globular domain flanked by the PLP2 in N-terminal and a hydrophobic domain in C-terminal.

A total of 19 proteins/domains were used in our screening matrix. Out of the 361 protein pairs tested in the yeast two-hybrid analysis, 15 combinations produced a positive result, accounting for 4% of the possible protein interactions (Fig. 2). In comparison, about 6% of nonstructural protein–protein interactions were positive in the von Brunn et al. (2007) Y2H study. Surprisingly, no interaction is common to both studies. This discrepancy could be explained by the fact that two-hybrid false positives may arise in two-hybrid arrays and by the difference between the Y2H systems used (Uetz, 2002). With our Y2H system, to eliminate potential false-positive interaction, three different phenotypes were assessed (β -galactosidase, His and Ura) and the transcription from each reporter gene (LacZ, HIS3 and URA3) is driven by independent promoters. At last, we have considered an interaction as positive if at least one phenotype in 2 out of the 3 matrix experiments was positive.

3.1.1. Identification of multiple interactions for nsp3 and nsp14

Two SARS-CoV proteins (nsp3 and nsp14) were found to be involved in interactions with 4 or more partners. Domains from nsp3 interacted with nsp5, nsp6, nsp12, nsp13, nsp14 and nsp16, and in particular for the PLnc subdomain the unexpectedly large number of 5 interaction partners was identified. Since this domain is comprised of only 386 amino acids, it is tempting to speculate that it might sequentially interact with these partners rather than with all of them simultaneously. Consequently, nsp3 may serve as one of the RTC scaffolding proteins by bringing several nsps into close proximity of each other. The presence of a transmembrane domain within nsp3, and the observed interaction with the nsp6 transmembrane protein, reinforces the hypothesis of a membrane-associated scaffolding function for nsp3 in the infected cell. The nsp3 central role was not so clear in the von Brunn et al. (2007) study because nsp3 protein was subdivided only into two fragments (nt 2719–4431 and nt 4885–8484), splitting the SUD domain in two.

The nsp14 protein is an exoribonuclease playing an elusive, yet essential, role in the SARS-CoV life cycle (Minskaia et al., 2006). In addition to its interaction with nsp3, nsp14 interacted strongly with both nsp10, a protein with two zinc-fingers potentially involved in nucleic acid recognition, and nsp16, the 2'-O-ribose methyltransferase. Interestingly, the interactions between nsp10, nsp14 and nsp16 were the only reciprocal ones, meaning that they were also detected when the DB and AD fusion partners were swapped. It is tempting to speculate that these three proteins form a complex that is associated with nsp3 and that the other interactions that were detected may reflect different and/or alternative complexes existing at different time points. The surface of interaction of nsp10 with nsp16 was mapped by reverse yeast two-hybrid system and in mammalian

cells, using the bioluminescence resonance energy transfer technology (BRET). Point mutations that abrogate the nsp10–nsp16 interaction also inhibit the interaction between nsp10 and nsp14, albeit with subtle differences, suggesting that the interacting surface is overlapping (PL, unpublished data). Two crystal structures were available for nsp10. One of them reveals a unique spherical dodecamer architecture (Su et al., 2006) and the other shows a monomer (Joseph et al., 2006). nsp10 protein is able to bind single- and double-stranded RNA and DNA without apparent sequence specificity (Joseph et al., 2006) and was suggested to be involved in SARS-CoV replication based on structural similarities with nuclear proteins (Su et al., 2006). The overall positive charge of the inner and outer surfaces of the dodecamer would be compatible with an RNA-binding function. Interestingly, nsp10 also interacts with nsp9, a single-stranded RNA binding protein (Egloff et al., 2004; Su et al., 2006; Sutton et al., 2004) that in turn interacts with nsp8, the putative RNA primase (Imbert et al., 2006).

In human coronavirus 229E, mutagenesis of the active site of the nsp14 exonuclease greatly reduced the accumulation of viral RNA, suggesting an essential role for this enzyme in replication and transcription (Minskaia et al., 2006). This critical function of nsp14 was also supported by results obtained with a SARS-CoV replicon, in a study that also addressed the impact of mutations within or deletion of nsp15- and nsp16-coding sequences, clearly demonstrating that these proteins are required for efficient replication (Almazan et al., 2006). Finally, by interacting with nsp3 through the PLnc domain, and with nsp7, nsp9 and nsp10, the nsp14 exoribonuclease may also be a key RTC scaffolding component, irrespective of its nucleic acid binding activity.

3.1.2. One-on-one interactions

A number of nsps (nsp1, nsp13, and nsp15) interacted with a single partner and these interactions were only detected when they were used as prey (Fig. 2). SARS-CoV nsp1, a small protein (Almeida et al., 2007), unique to SARS-CoV, believed to be involved in host cell RNA degradation, may not directly participate in viral RNA synthesis. Consequently, it may be not too surprising that its only interaction partner was nsp9, a single-stranded RNA binding protein that, in turn, was not densely connected to other nsps (Fig. 2).

In the case of the large nsp13 and nsp15 subunits, it is impossible at this stage to assess whether their size (or any other factor) may have impeded their expression or correct folding in yeast, thus preventing detection of protein–protein interaction in the yeast two-hybrid system. Alternatively, the toxicity of RNA-modifying enzymes that is often observed when they are expressed as recombinant proteins may have played a role. nsp13 and nsp15 could also belong to larger hetero-multimers, like the nsp7–nsp8 complex. Notably, and despite the documented interaction of nsp8 with nsp7, nsp15 and nsp8 formed the sole isolated protein pair. We failed to detect nsp10 dimerization in the yeast-two hybrid system, as in the von Brunn et al. (2007) study, even though one of the two crystal structures reveals a dodecameric arrangement based on nsp10–nsp10 interactions (Su et al., 2006). The second crystal structure shows a

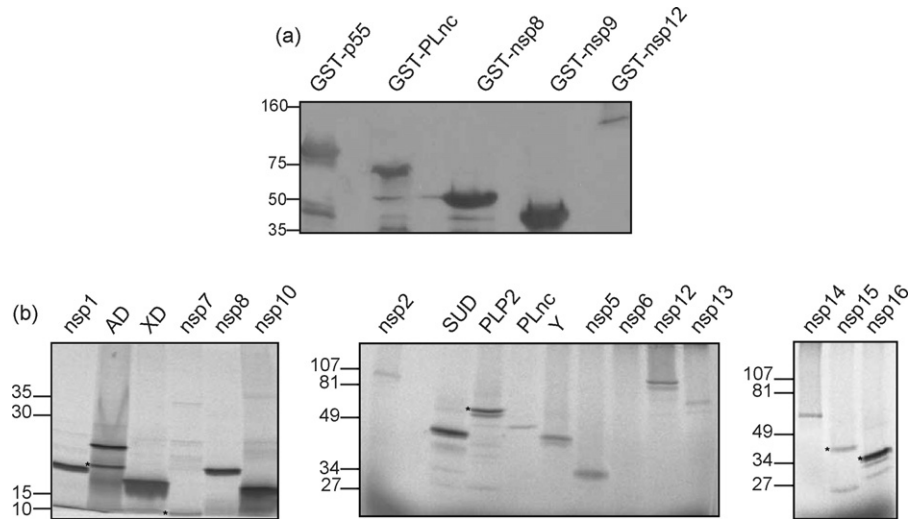


Fig. 3. (a) Immunoblot analysis of purified, glutathione-sepharose-immobilized GST-p55, GST-PLnc, GST-nsp8, GST-nsp9, and GST-nsp12. Samples of glutathione-sepharose bound, bacterially expressed were analyzed by SDS-PAGE followed by immunoblotting with an anti-GST antibody. For the GST-nsp12 sample, material derived from 20 times more bacteria was loaded. (b) Autoradiogram from SDS-PAGE analysis of *in vitro* translated SARS-CoV nonstructural proteins. [35 S]Methionine-labelled samples were subjected to SDS-PAGE and autoradiography. Positions of molecular size standards are indicated on the left side, in kilodaltons. When additional products are visible in the gel, the band of the expected size is indicated with a star.

monomer (Joseph et al., 2006). The dodecamer supercomplex may lack biological relevance, because the second zinc-finger lacks the last cysteine residue and the remainder of the C-terminal tail is disordered. Unexpectedly also, in particular since helicases are known to interact with RdRps in RTCs (Dimitrova et al., 2003; Piccininni et al., 2002), the nsp13 helicase stood alone and interactions between nsp12 and nsp13 were not detected.

3.1.3. Interaction orphans

In the yeast two-hybrid matrix screening, a number of proteins did not interact with any other nsp or subdomain. These were nsp2 and the XD, SUD and Y domains of nsp3. It is interesting to note that nsp2, which appears to be unique to SARS-CoV, is dispensable for replication and transcription (Graham et al., 2005). Also, the ADP-ribose-1''-monophosphatase (ADRP) activity of the XD subdomain was found to be dispensable for

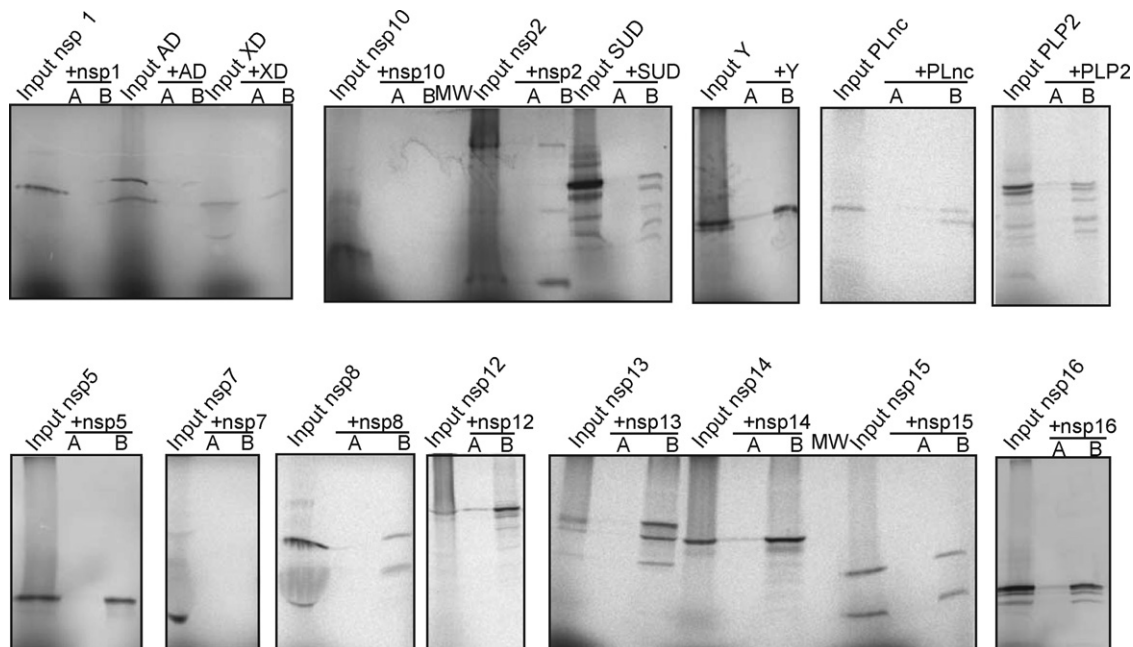


Fig. 4. GST pull-down analysis to identify interaction partners of nsp12-RdRp. Each panel shows an autoradiogram from a SDS-PAGE analysis of *in vitro*-translated nonstructural proteins pulled down by binding to either glutathione-sepharose-bound GST-p55 (negative control; lanes A) or GST-nsp12 (lanes B). Equal amounts of [35 S]methionine-labelled target were used for lanes (A and B) and the input material was also run next to the pull-down samples, as indicated for each panel.

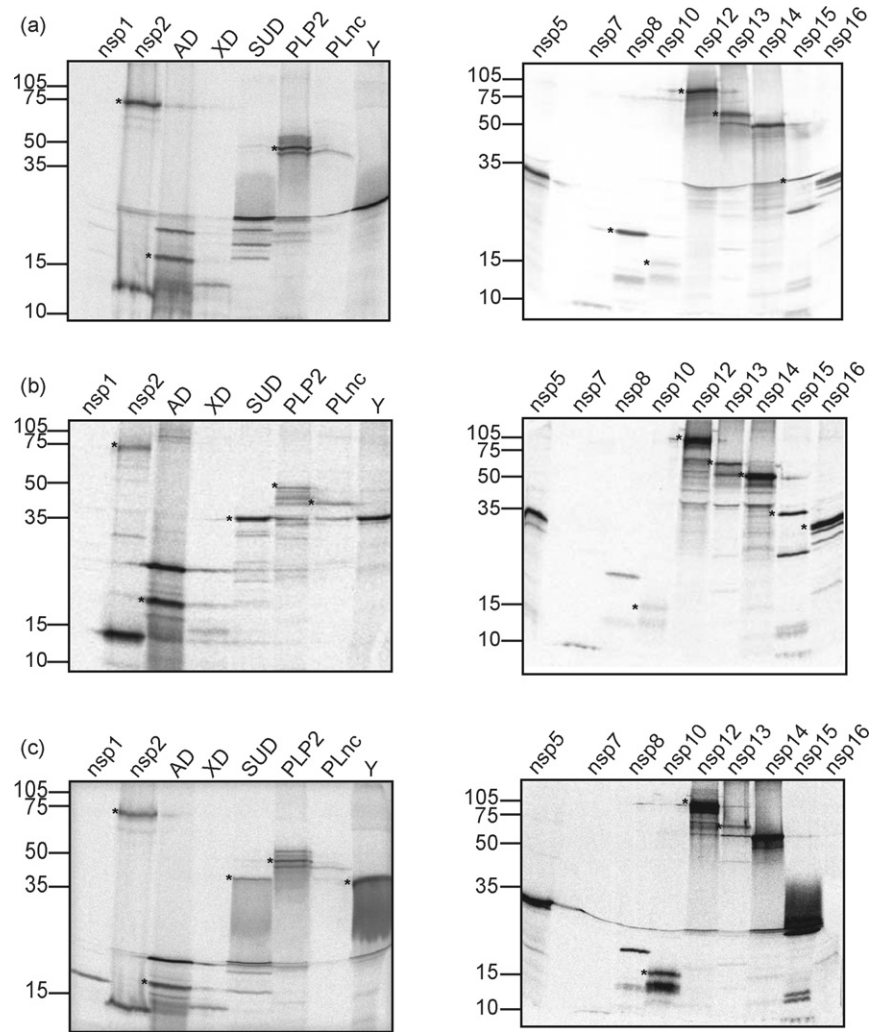


Fig. 5. GST pull-down analysis using nsp8 (a), the nsp3 PLnc domain (b), and nsp9 (c) as bait. Each panel shows an autoradiogram from a SDS-PAGE 12% analysis of *in vitro*-translated nsps brought down by binding (a) GST-nsp8, (b) GST-PLnc and (c) GST-nsp9. Positions of molecular size standards are indicated on the left side, in kilodaltons. When additional products are visible in the gel, the band of the expected size is indicated with a star.

coronavirus replication (Putics et al., 2005). The SUD domain binds oligo(G) stretches and may be involved in the modulation of host-cell signalling pathways (Tan et al., in press). Finally, the Y domain of nsp3 has no obvious role in RNA synthesis. Therefore, it is logical to propose that they may rather play a role in virus-host interactions to, e.g. modulate immunity and/or pathogenesis.

3.1.4. Few interactions for the RNA-dependent RNA polymerase (nsp12)

Surprisingly, despite its presumed central role in RNA synthesis, the nsp12-RdRp was found to interact with only two other nsps, namely nsp7 and nsp3. nsp7–nsp8 could be part of a larger complex including nsp12 on the one hand and nsp14, nsp9 and nsp10 on the other (Fig. 2). These results also reflected the potential limitations of the yeast-two-hybrid approach when analyzing large proteins like nsp12, prompting us to develop an alternative to confirm and/or extend our interaction map.

3.2. GST pull-down analysis

It is well-known that – for technical reasons – yeast two-hybrid screening may not reveal all interactions that normally occur in a cellular environment, owing, e.g. to steric hindrance of the fusion partners used in yeast two-hybrid assays or the inability of certain fusion proteins to be expressed and targeted to the yeast nucleus. Therefore, as an additional approach to identify potential interactions of the PLnc domain, nsp8, nsp9 and nsp12-RdRp with other SARS-CoV nsps, we carried out a set of pull-down assays using GST fusion proteins. This type of assay can be used to analyze the binding of a radiolabeled, *in vitro*-translated protein to an interaction partner presented in the form of a purified GST fusion protein bound to glutathione-sepharose beads. GST fusion proteins, as well as a HIV-1 gag fusion protein (GST-p55) that was used as negative control, were expressed in *E. coli* and immobilized on glutathione-sepharose beads (Fig. 3a). GST-p55, GST-PLnc, GST-nsp8 and GST-nsp9 were much more soluble in bacteria

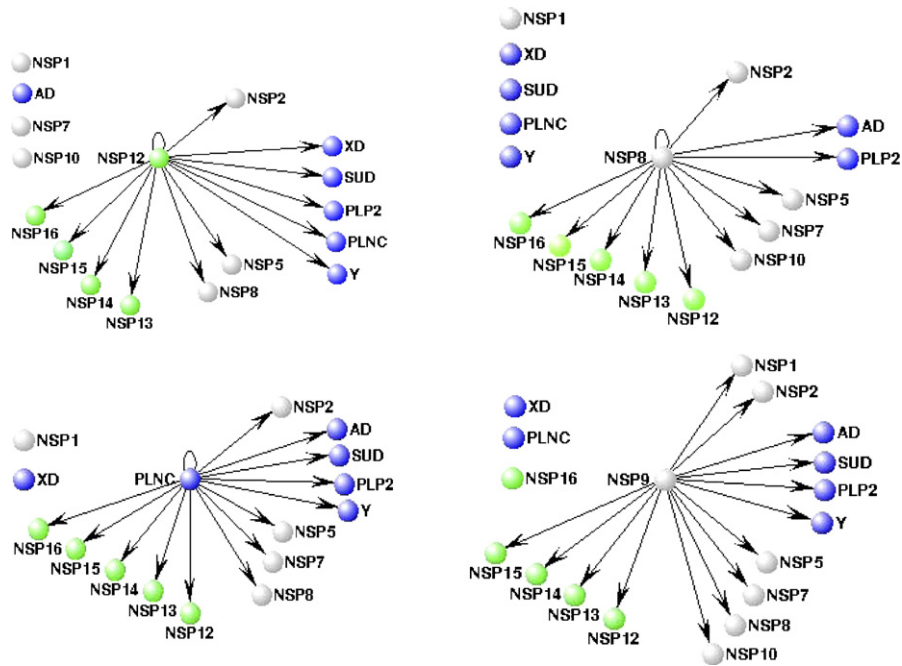


Fig. 6. Schematic summary of GST pull-down results. Nodes in blue and green represent nsp3 domains and ORF1b-encoded proteins, respectively. Proteins that did not interact with the bait are depicted at the left side of each diagram.

than GST-nsp12 and could be purified in considerably larger amounts (Fig. 3a). Therefore, only 1/50 of a standard GST-p55, GST-nsp8 and GST-nsp9 preparation was used in the assays, whereas the complete yield of a GST-nsp12 purification was used (Fig. 3a). To obtain potential interaction partners, not containing any foreign tags, all SARS-CoV nsps and domains used before (Table 1) were *in vitro* translated in the presence of [³⁵S]-labelled methionine, except for nsp4 (an integral transmembrane domain) and nsp11 (which is only 13 amino acids long) (Fig. 3b). Despite repeated attempts, we could not achieve the expression of nsp6 and nsp9 in the TNT T7-coupled reticulocyte lysate system. The *in vitro* synthesis of full-length proteins was confirmed by SDS-PAGE analysis (Fig. 3b). A few truncated products were observed for the SUD, PLP2, nsp15 and nsp16 proteins. The AD protein corresponds to the lower band on the different gels, according to the protein molecular weight marker. We do not have an explanation regarding the other higher band observed for AD. nsp2 protein (70 kDa) appears to migrate more slowly than nsp12 protein (102 kDa) (Fig. 3b, middle panel). This discrepancy may be related to the amino-terminal part of nsp2 protein which appears to be disordered. It is documented that disordered protein might have an atypical migration pattern, which is variable according to the percentage of acrylamide sieving. GST pull-down assays were carried out with approximately equimolar levels of input material.

3.2.1. GST pull-down experiments identify multiple interaction partners for nsp12-RdRp

Pull-down assays with GST-nsp12 revealed that the SARS-CoV RdRp does not interact with nsp1, AD, nsp7, or nsp10 (Figs. 4 and 6). Interactions between GST-nsp12 and nsp2, XD,

SUD, PLnc, PLP2, and nsp8 were detected, in the absence of a signal for the GST-p55 negative control (Fig. 4, lanes B). Interactions were also observed with the nsp3-Y domain, nsp5, nsp13, nsp14, nsp15 and nsp16. nsp3-Y domain, nsp12, nsp14 and nsp16 also showed a weak interaction with GST-p55 (Fig. 4, lanes A) and GST alone (not shown), but the signal clearly increased when specific SARS-CoV GST-nsp fusion proteins were used. Therefore, these background signals were attributed to the large amount of the control proteins used in comparison with the amount of GST-nsp12. In contrast to the yeast two-hybrid analysis, GST-nsp12 failed to interact with nsp7. The same interactions were detected after RNase treatment of the *in vitro* translation products used for these binding studies, indicating that the observed interactions were not mediated by RNA (data not shown).

From these GST pull-down experiments with nsp12-RdRp, a clear pattern emerged: the RdRp-containing subunit is apparently able to build two interactomes: one with nsp3 domains and the other with products encoded by ORF1b, which had been missed in the yeast two-hybrid experiments. Notably, nsp12 is also able to dimerize, perhaps providing an explanation for the fact that many interactions involving nsp12 were missed using the yeast two hybrid system (see also below). The nsp12–nsp7 interaction could not be reproduced using the GST pull-down approach. The negative results for nsp1, AD, and nsp10 were consistent with the yeast two-hybrid data.

3.2.2. Overlapping interaction profiles for nsp8 and nsp12

The recently discovered primase activity of nsp8 made this protein a very interesting bait for an extended interaction analysis. The interaction pattern of GST-nsp8 was found to be related to that of GST-nsp12 (Fig. 6). Although interactions with mul-

multiple nsp3 subdomains (XD, SUD, PLnc and Y) were missing, nsp2, PLP2, nsp5 and ORF1b-encoded products, were identified as interactors, yielding the same interaction tree obtained for GST-nsp12. The bands corresponding to SUD and Y domains did not migrate to the expected distance but much lower further (Fig. 5a, left panel). For the SUD domain, a strong tendency to proteolytic (self-)degradation was shown by others (Tan et al., *in press*). However, this discrepancy in size was not observed with the GST-PLnc pull-down assay (see below). Furthermore, these experiments confirmed the nsp8/nsp15 interaction previously identified by yeast two-hybrid screening (Fig. 2) and revealed that nsp8 dimerized, in accordance with structural, biochemical, and enzymatic data (Imbert et al., 2006; Zhai et al., 2005).

3.2.3. Confirmation of the large number of interactions of the nsp3 PLnc domain

The yeast two-hybrid screening (Fig. 2) identified the nsp3 PLnc domain as a central interactor in the SARS-CoV RTC. Thus, PLnc pull-down assays were performed in order to confirm and perhaps extend these findings. Indeed, this alternative assay confirmed interactions of PLnc with nsp5, nsp12, nsp13, nsp14 and nsp16 (Figs. 5b and 6). Moreover, additional interactions were revealed with nsp2, several nsp3 subdomains (AD, SUD, PLP2 and Y), nsp7, nsp8 and nsp15. Taken together, these data supported the previously proposed scaffolding role for nsp3, in which the PLnc subdomain may fulfill a central organizing position.

3.2.4. An unusually large number of interactions for nsp9

For unknown reasons, nsp9 expression in the TNT T7-coupled reticulocyte lysate system remained unsuccessful. Therefore, a GST-nsp9 fusion protein was produced and used to complete our interaction screening. GST-nsp9 interacted with nsp1, nsp2, some nsp3 domains (AD, SUD, PLP2, Y), nsp5, nsp7, nsp8, nsp10, nsp12, nsp13, nsp14 and nsp15 (Figs. 5c and 6). Overall, like the nsp3 PLnc domain, nsp9 seems to have many partners and interacts with almost all nsps except for nsp16. The GST-nsp9 pull-down analysis confirmed the interactions identified above in the yeast two-hybrid approach (nsp9 with nsp1 and nsp14) and also the previously documented nsp9–nsp10 interaction (Su et al., 2006). Both are RNA-binding proteins that may cooperate at some point in the virus life cycle. The nsp10/GST-nsp8 interaction and the nsp10/GST-PLnc interaction are much weaker than nsp10/GST–nsp9 interaction.

4. Conclusion

In this study, we investigated *in vitro* and *in cellulo* the network of interactions that must exist amongst the viral proteins that assemble into the SARS-CoV RTC. These data may enhance our understanding of coronavirus replication and transcription at the molecular level. We have not only confirmed interactions previously deduced from a variety of experimental approaches, but have also identified a significant number of previously unknown (potential) interactions between SARS-CoV replicase cleavage products or domains. In the first place, we have provided evi-

dence for physical interactions that may be the basis for the previously described co-localization of various key enzymes of the SARS-CoV RTC in infected cells (nsp3, nsp5, nsp12, nsp13 and nsp15; Snijder et al., 2006). Co-immunoprecipitation in mammalian 293 cells confirmed interactions of nsp8 with nsp2, nsp7, nsp8, nsp9, nsp12, nsp13 and nsp14 (von Brunn et al., 2007) and highlighted its central role within the RTC machinery.

Secondly, the nsp3 PLnc domain, nsp8 and nsp12 were able to form stable homodimers. Thirdly, the nsp8/nsp15 interactions initially detected by yeast two-hybrid screening could be confirmed in GST pull-down assays. Previously described nsp8/nsp9/nsp10 interactions (Su et al., 2006; Sutton et al., 2004) were also confirmed in the latter assay (Fig. 5, panels a and c). Finally, three viral interaction partners for nsp2 (nsp8, nsp9 and nsp12) were identified in the pull-down analysis, although the yeast two-hybrid analysis had not revealed these interactions.

The coronavirus RTC engages in a variety of RNA synthesis processes with replication and sg mRNA synthesis each proceeding through their specific minus-strand templates. How the RTC accomplishes and balances these various processes remains to be elucidated. It is unknown whether complexes with different composition exist that are specifically dedicated to, e.g. replication or transcription. Alternatively, one type of complex may be converted into another by the binding or release of specific protein partners. In this manner, such protein factors may regulate the balance between replication and transcription, if carried out by the same complex, or direct the formation of specialized “replicase” and “transcriptase” complexes. The molecular mechanism and factors governing this switch in coronaviruses are unknown. In the related arterivirus system, nsp1 was identified as a clear example of a protein with a transcription-specific function. Deletion of this replicase subunit did not affect replication, but reduced sg mRNA synthesis to undetectable levels (Tijms et al., 2001). In alphaviruses, temporal regulation of replicase polyprotein cleavage by the nsP2 protease was found to be a key factor in regulating the switch from minus- to plus-strand RNA synthesis (Kaariainen and Ahola, 2002; Lemm et al., 1994), illustrating another barely explored feature of the nidovirus/coronavirus system: replicase subunits may act either after complete maturation, or as part of larger processing intermediates, or both. Thus, RTC function may be temporally and spatially coordinated by the activity of the protease domains embedded in replicase polyproteins.

Our interactome studies confirmed that the key enzymes encoded by replicase ORF1b likely exist as a complex, which may be organized around the dimerizing nsp12-RdRp. It is unknown whether dimerization is essential for RdRp activity, as, e.g. in the case of hepatitis C virus (Qin et al., 2002). In general, RdRp error frequencies are estimated to be in the order of 10^{-4} (Huang et al., 2000). For many years, this number, in combination with the unusual size of the coronavirus genome, has triggered speculations about the presence of proofreading or other repair mechanisms. The GST-nsp12 pull-down experiments identified nsp13 to nsp16 as strong interactors (Fig. 4), and the fact that this pattern overlaps with that of the nsp8-primase is intriguing (Fig. 5a). The interaction of these proteins,

either simultaneously or successively, with the helicase (nsp13), 3' → 5' exonuclease (nsp14), endonuclease (nsp15) and (putative) methyltransferase (nsp16) supports the hypothesis that these subunits may mediate successive steps of the same pathway (Snijder et al., 2003) and provides a basis for further experiments aimed at, for example, exploring the existence of a proofreading mechanism. It is interesting to note that the nsp13 helicase, with a 5'–3' directionality, appears to lack interactions with nsp14, nsp15 and nsp16 (our study and von Brunn et al., 2007). In flaviviruses, NS3 helicase unwinds its substrates in a 3'-to-5' direction and physical mapping and structural studies indicate that the helicase most likely precedes the NS5 RdRp undergoing RNA synthesis (Malet et al., 2007). Upon isolation of an active coronavirus RdRp, it will be interesting to determine if this is also the case in coronaviruses, in view of the different RNA unwinding polarities (Patel and Donmez, 2006).

In conclusion, our work confirms and defines several association groups among SARS-CoV nsps that will provide a basis to investigate cooperative enzymatic functions as well as currently unknown tertiary and quaternary structures. In this manner, these data may also contribute to the development of *in vitro* assays faithfully reproducing the different steps in coronavirus RNA synthesis. Furthermore, compounds affecting interactions between essential components of the RTC may inhibit enzymatic activities and may thus provide novel perspectives for antiviral drug design.

Acknowledgements

We thank Andrew Davidson and John Ziebuhr for helpful discussion and sharing preliminary data. We acknowledge Jessika Zevenhoven-Dobbe, François Ferron, Christian Cambillau, Valérie Campanacci and Sonia Longhi for material and their help in the initial phase of the project. We thank Claire Debarnot, Etienne Decroly and Bruno Coutard for excellent technical assistance. Dr. J.P. Borg is greatly acknowledged for lab space, equipment, and funding to P.L.

This work was supported by the Structural Proteomics in Europe (SPINE) project of the European Union 5th framework research program (Grant QLRT-2001-00988) and subsequently by the Euro-Asian SARS-DTV Network (SP22-CT-2004-511064) from the European Commission specific research and technological development Programme “Integrating and strengthening the European Research area” and partially by Interdisciplinary CNRS 2007 program “Infectious Emerging Diseases”.

References

Almazan, F., Dediego, M.L., Galan, C., Escors, D., Alvarez, E., Ortego, J., Sola, I., Zuniga, S., Alonso, S., Moreno, J.L., Nogales, A., Capiscol, C., Enjuanes, L., 2006. Construction of a severe acute respiratory syndrome coronavirus infectious cDNA clone and a replicon to study coronavirus RNA synthesis. *J. Virol.* 80 (21), 10900–10906.

Almeida, M.S., Johnson, M.A., Herrmann, T., Gerecht, M., Wuthrich, K., 2007. Novel beta-barrel fold in the nuclear magnetic resonance structure of the replicase nonstructural protein 1 from the severe acute respiratory syndrome coronavirus. *J. Virol.* 81 (7), 3151–3161.

Anand, K., Ziebuhr, J., Wadhvani, P., Mesters, J.R., Hilgenfeld, R., 2003. Coronavirus main proteinase (3CLpro) structure: basis for design of anti-SARS drugs. *Science* 300 (5626), 1763–1767.

Barretto, N., Jukneliene, D., Ratia, K., Chen, Z., Mesecar, A.D., Baker, S.C., 2005. The papain-like protease of severe acute respiratory syndrome coronavirus has deubiquitinating activity. *J. Virol.* 79 (24), 15189–15198.

Bhardwaj, K., Sun, J., Holzenburg, A., Guarino, L.A., Kao, C.C., 2006. RNA recognition and cleavage by the SARS coronavirus endoribonuclease. *J. Mol. Biol.* 361 (2), 243–256.

Bost, A.G., Prentice, E., Denison, M.R., 2001. Mouse hepatitis virus replicase protein complexes are translocated to sites of M protein accumulation in the ERGIC at late times of infection. *Virology* 285 (1), 21–29.

Brierley, I., Dos Ramos, F.J., 2006. Programmed ribosomal frameshifting in HIV-1 and the SARS-CoV. *Virus Res.* 119 (1), 29–42.

Brierley, I., Digard, P., Inglis, S.C., 1989. Characterization of an efficient coronavirus ribosomal frameshifting signal: requirement for an RNA pseudoknot. *Cell* 57 (4), 537–547.

Cheng, A., Zhang, W., Xie, Y., Jiang, W., Arnold, E., Sarafianos, S.G., Ding, J., 2005. Expression, purification, and characterization of SARS coronavirus RNA polymerase. *Virology* 335 (2), 165–176.

Dimitrova, M., Imbert, I., Kieny, M.P., Schuster, C., 2003. Protein–protein interactions between hepatitis C virus nonstructural proteins. *J. Virol.* 77 (9), 5401–5414.

Douaisi, M., Dussart, S., Courcoul, M., Bessou, G., Vigne, R., Decroly, E., 2004. HIV-1 and MLV Gag proteins are sufficient to recruit APOBEC3G into virus-like particles. *Biochem. Biophys. Res. Commun.* 321 (3), 566–573.

Drosten, C., Gunther, S., Preiser, W., van der Werf, S., Brodt, H.R., Becker, S., Rabenau, H., Panning, M., Kolesnikova, L., Fouchier, R.A., Berger, A., Burguiere, A.M., Cinatl, J., Eickmann, M., Escρίου, N., Grywna, K., Kramme, S., Manuguerra, J.C., Müller, S., Rickerts, V., Stürmer, M., Vieth, S., Klenk, H.D., Osterhaus, A.D., Schmitz, H., Doerr, H.W., 2003. Identification of a novel coronavirus in patients with severe acute respiratory syndrome. *N. Engl. J. Med.* 348 (20), 1967–1976.

Egloff, M.P., Ferron, F., Campanacci, V., Longhi, S., Rancurel, C., Dutartre, H., Snijder, E.J., Gorbalenya, A.E., Cambillau, C., Canard, B., 2004. The severe acute respiratory syndrome-coronavirus replicative protein nsp9 is a single-stranded RNA-binding subunit unique in the RNA virus world. *Proc. Natl. Acad. Sci. U.S.A.* 101 (11), 3792–3796.

Egloff, M.P., Malet, H., Putics, A., Heinonen, M., Dutartre, H., Frangeul, A., Gruez, A., Campanacci, V., Cambillau, C., Ziebuhr, J., Ahola, T., Canard, B., 2006. Structural and functional basis for ADP-ribose and poly(ADP-ribose) binding by viral macro domains. *J. Virol.* 80 (17), 8493–8502.

Ferron, F., Rancurel, C., Longhi, S., Cambillau, C., Henrissat, B., Canard, B., 2005. VaZyMoLo: a tool to define and classify modularity in viral proteins. *J. Gen. Virol.* 86 (Pt 3), 743–749.

Gorbalenya, A.E., Koonin, E.V., Donchenko, A.P., Blinov, V.M., 1989. Coronavirus genome: prediction of putative functional domains in the non-structural polyprotein by comparative amino acid sequence analysis. *Nucleic Acids Res.* 17 (12), 4847–4861.

Gorbalenya, A.E., Enjuanes, L., Ziebuhr, J., Snijder, E.J., 2006. Nidovirales: evolving the largest RNA virus genome. *Virus Res.* 117 (1), 17–37.

Gosert, R., Kanjanahaluethai, A., Egger, D., Bienz, K., Baker, S.C., 2002. RNA replication of mouse hepatitis virus takes place at double-membrane vesicles. *J. Virol.* 76 (8), 3697–3708.

Graham, R.L., Sims, A.C., Brockway, S.M., Baric, R.S., Denison, M.R., 2005. The nsp2 replicase proteins of murine hepatitis virus and severe acute respiratory syndrome coronavirus are dispensable for viral replication. *J. Virol.* 79 (21), 13399–13411.

Harcourt, B.H., Jukneliene, D., Kanjanahaluethai, A., Bechill, J., Severson, K.M., Smith, C.M., Rota, P.A., Baker, S.C., 2004. Identification of severe acute respiratory syndrome coronavirus replicase products and characterization of papain-like protease activity. *J. Virol.* 78 (24), 13600–13612.

Huang, J., Briebe, L.G., Sousa, R., 2000. Misincorporation by wild-type and mutant T7 RNA polymerases: identification of interactions that reduce misincorporation rates by stabilizing the catalytically incompetent open conformation. *Biochemistry* 39 (38), 11571–11580.

- Imbert, I., Guillemot, J.C., Bourhis, J.M., Bussetta, C., Coutard, B., Egloff, M.P., Ferron, F., Gorbalenya, A.E., Canard, B., 2006. A second, non-canonical RNA-dependent RNA polymerase in SARS coronavirus. *EMBO J.* 25 (20), 4933–4942.
- Ivanov, K.A., Hertzog, T., Rozanov, M., Bayer, S., Thiel, V., Gorbalenya, A.E., Ziebuhr, J., 2004a. Major genetic marker of nido viruses encodes a replicative endoribonuclease. *Proc. Natl. Acad. Sci. U.S.A.* 101 (34), 12694–12699.
- Ivanov, K.A., Thiel, V., Dobbe, J.C., van der Meer, Y., Snijder, E.J., Ziebuhr, J., 2004b. Multiple enzymatic activities associated with severe acute respiratory syndrome coronavirus helicase. *J. Virol.* 78 (11), 5619–5632.
- Joseph, J.S., Saikatendu, K.S., Subramanian, V., Neuman, B.W., Brooun, A., Griffith, M., Moy, K., Yadav, M.K., Velasquez, J., Buchmeier, M.J., Stevens, R.C., Kuhn, P., 2006. Crystal structure of nonstructural protein 10 from the severe acute respiratory syndrome coronavirus reveals a novel fold with two zinc-binding motifs. *J. Virol.* 80 (16), 7894–7901.
- Kaariainen, L., Ahola, T., 2002. Functions of alphavirus nonstructural proteins in RNA replication. *Prog. Nucleic Acid Res. Mol. Biol.* 71, 187–222.
- Kamitani, W., Narayanan, K., Huang, C., Lokugamage, K., Ikegami, T., Ito, N., Kubo, H., Makino, S., 2006. Severe acute respiratory syndrome coronavirus nsp1 protein suppresses host gene expression by promoting host mRNA degradation. *Proc. Natl. Acad. Sci. U.S.A.* 103 (34), 12885–12890.
- Kanjanahaluethai, A., Chen, Z., Jukneliene, D., Baker, S.C., 2007. Membrane topology of murine coronavirus replicase nonstructural protein 3. *Virology* 361 (2), 391–401.
- Ksiazek, T.G., Erdman, D., Goldsmith, C.S., Zaki, S.R., Peret, T., Emery, S., Tong, S., Urbani, C., Comer, J.A., Lim, W., Rollin, P.E., Dowell, S.F., Ling, A.E., Humphrey, C.D., Shieh, W.J., Guarner, J., Paddock, C.D., Rota, P., Fields, B., DeRisi, J., Yang, J.Y., Cox, N., Hughes, J.M., LeDuc, J.W., Bellini, W.J., Anderson, L.J., 2003. A novel coronavirus associated with severe acute respiratory syndrome. *N. Engl. J. Med.* 348 (20), 1953–1966.
- Law, A.H., Lee, D.C., Cheung, B.K., Yim, H.C., Lau, A.S., 2007. Role for nonstructural protein 1 of severe acute respiratory syndrome coronavirus in chemokine dysregulation. *J. Virol.* 81 (1), 416–422.
- Lemm, J.A., Rumenapf, T., Strauss, E.G., Strauss, J.H., Rice, C.M., 1994. Polypeptide requirements for assembly of functional Sindbis virus replication complexes: a model for the temporal regulation of minus- and plus-strand RNA synthesis. *EMBO J.* 13 (12), 2925–2934.
- Lindner, H.A., Fotouhi-Ardakani, N., Lytvyn, V., Lachance, P., Sulea, T., Menard, R., 2005. The papain-like protease from the severe acute respiratory syndrome coronavirus is a deubiquitinating enzyme. *J. Virol.* 79 (24), 15199–15208.
- Mackenzie, J., 2005. Wrapping things up about virus RNA replication. *Traffic* 6 (11), 967–977.
- Malet, H., Egloff, M.P., Selisko, B., Butcher, R.E., Wright, P.J., Roberts, M., Gruez, A., Sulzenbacher, G., Vornrhein, C., Bricogne, G., Mackenzie, J.M., Khromykh, A.A., Davidson, A.D., Canard, B., 2007. Crystal structure of the RNA polymerase domain of the West Nile virus non-structural protein 5. *J. Biol. Chem.* 282 (14), 10678–10689.
- Marra, M.A., Jones, S.J., Astell, C.R., Holt, R.A., Brooks-Wilson, A., Butterfield, Y.S., Khattri, J., Asano, J.K., Barber, S.A., Chan, S.Y., Cloutier, A., Coughlin, S.M., Freeman, D., Girm, N., Griffith, O.L., Leach, S.R., Mayo, M., McDonald, H., Montgomery, S.B., Pandoh, P.K., Petrescu, A.S., Robertson, A.G., Schein, J.E., Siddiqui, A., Smailus, D.E., Stott, J.M., Yang, G.S., Plummer, F., Andonov, A., Artsob, H., Bastien, N., Bernard, K., Booth, T.F., Bowness, D., Czub, M., Drebot, M., Fernando, L., Flick, R., Garbutt, M., Gray, M., Grolla, A., Jones, S., Feldmann, H., Meyers, A., Kabani, A., Li, Y., Normand, S., Stroher, U., Tipples, G.A., Tyler, S., Vogrig, R., Ward, D., Watson, B., Brunham, R.C., Krajden, M., Petric, M., Skowronski, D.M., Upton, C., Roper, R.L., 2003. The genome sequence of the SARS-associated coronavirus. *Science* 300 (5624), 1399–1404.
- Matthes, N., Mesters, J.R., Coutard, B., Canard, B., Snijder, E.J., Moll, R., Hilgenfeld, R., 2006. The non-structural protein nsp10 of mouse hepatitis virus binds zinc ions and nucleic acids. *FEBS Lett.* 580 (17), 4143–4149.
- Minskaia, E., Hertzog, T., Gorbalenya, A.E., Campanacci, V., Cambillau, C., Canard, B., Ziebuhr, J., 2006. Discovery of an RNA virus 3′ → 5′ exoribonuclease that is critically involved in coronavirus RNA synthesis. *Proc. Natl. Acad. Sci. U.S.A.* 103 (13), 5108–5113.
- Pasternak, A.O., Spaan, W.J., Snijder, E.J., 2006. Nidovirus transcription: how to make sense? *J. Gen. Virol.* 87 (Pt 6), 1403–1421.
- Patel, S.S., Donmez, I., 2006. Mechanisms of helicases. *J. Biol. Chem.* 281 (27), 18265–18268.
- Peiris, J.S., Lai, S.T., Poon, L.L., Guan, Y., Yam, L.Y., Lim, W., Nicholls, J., Yee, W.K., Yan, W.W., Cheung, M.T., Cheng, V.C., Chan, K.H., Tsang, D.N., Yung, R.W., Ng, T.K., Yuen, K.Y., 2003. Coronavirus as a possible cause of severe acute respiratory syndrome. *Lancet* 361 (9366), 1319–1325.
- Piccininni, S., Varaklioti, A., Nardelli, M., Dave, B., Raney, K.D., McCarthy, J.E., 2002. Modulation of the hepatitis C virus RNA-dependent RNA polymerase activity by the non-structural (NS) 3 helicase and the NS4B membrane protein. *J. Biol. Chem.* 277 (47), 45670–45679.
- Prentice, E., McAuliffe, J., Lu, X., Subbarao, K., Denison, M.R., 2004. Identification and characterization of severe acute respiratory syndrome coronavirus replicase proteins. *J. Virol.* 78 (18), 9977–9986.
- Putics, A., Filipowicz, W., Hall, J., Gorbalenya, A.E., Ziebuhr, J., 2005. ADP-ribose-1′′-monophosphatase: a conserved coronavirus enzyme that is dispensable for viral replication in tissue culture. *J. Virol.* 79 (20), 12721–12731.
- Qin, W., Luo, H., Nomura, T., Hayashi, N., Yamashita, T., Murakami, S., 2002. Oligomeric interaction of hepatitis C virus NS5B is critical for catalytic activity of RNA-dependent RNA polymerase. *J. Biol. Chem.* 277 (3), 2132–2137.
- Ratia, K., Saikatendu, K.S., Santarsiero, B.D., Barretto, N., Baker, S.C., Stevens, R.C., Mesecar, A.D., 2006. Severe acute respiratory syndrome coronavirus papain-like protease: structure of a viral deubiquitinating enzyme. *Proc. Natl. Acad. Sci. U.S.A.* 103 (15), 5717–5722.
- Rota, P.A., Oberste, M.S., Monroe, S.S., Nix, W.A., Campagnoli, R., Icenogle, J.P., Penaranda, S., Bankamp, B., Maher, K., Chen, M.H., Tong, S., Tamin, A., Lowe, L., Frace, M., DeRisi, J.L., Chen, Q., Wang, D., Erdman, D.D., Peret, T.C., Burns, C., Ksiazek, T.G., Rollin, P.E., Sanchez, A., Liffick, S., Holloway, B., Limor, J., McCaustland, K., Olsen-Rasmussen, M., Fouchier, R., Gunther, S., Osterhaus, A.D., Drosten, C., Pallansch, M.A., Anderson, L.J., Bellini, W.J., 2003. Characterization of a novel coronavirus associated with severe acute respiratory syndrome. *Science* 300 (5624), 1394–1399.
- Saikatendu, K.S., Joseph, J.S., Subramanian, V., Clayton, T., Griffith, M., Moy, K., Velasquez, J., Neuman, B.W., Buchmeier, M.J., Stevens, R.C., Kuhn, P., 2005. Structural basis of severe acute respiratory syndrome coronavirus ADP-ribose-1′′-phosphate dephosphorylation by a conserved domain of nsP3. *Structure* 13 (11), 1665–1675.
- Salonen, A., Ahola, T., Kaariainen, L., 2004. Viral RNA replication in association with cellular membranes. *Curr. Top. Microbiol. Immunol.* 285, 139–173.
- Sawicki, S.G., Sawicki, D.L., 1995. Coronaviruses use discontinuous extension for synthesis of subgenome-length negative strands. *Adv. Exp. Med. Biol.* 380, 499–506.
- Sawicki, S.G., Sawicki, D.L., Younker, D., Meyer, Y., Thiel, V., Stokes, H., Siddell, S.G., 2005. Functional and genetic analysis of coronavirus replicase-transcriptase proteins. *PLoS Pathog.* 1 (4), e39.
- Sawicki, S.G., Sawicki, D.L., Siddell, S.G., 2007. A contemporary view of coronavirus transcription. *J. Virol.* 81 (1), 20–29.
- Serrano, P., Johnson, M.A., Almeida, M.S., Horst, R., Herrmann, T., Joseph, J.S., Neuman, B.W., Subramanian, V., Saikatendu, K.S., Buchmeier, M.J., Stevens, R.C., Kuhn, P., Wuthrich, K., 2007. Nuclear magnetic resonance structure of the N-terminal domain of nonstructural protein 3 from the severe acute respiratory syndrome coronavirus. *J. Virol.* 81 (21), 12049–12060.
- Seybert, A., Hegyi, A., Siddell, S.G., Ziebuhr, J., 2000. The human coronavirus 229E superfamily 1 helicase has RNA and DNA duplex-unwinding activities with 5′-to-3′ polarity. *RNA* 6 (7), 1056–1068.
- Seybert, A., Posthuma, C.C., van Dinten, L.C., Snijder, E.J., Gorbalenya, A.E., Ziebuhr, J., 2005. A complex zinc finger controls the enzymatic activities of nidovirus helicases. *J. Virol.* 79 (2), 696–704.
- Shi, S.T., Schiller, J.J., Kanjanahaluethai, A., Baker, S.C., Oh, J.W., Lai, M.M., 1999. Colocalization and membrane association of murine hepatitis virus gene 1 products and De novo-synthesized viral RNA in infected cells. *J. Virol.* 73 (7), 5957–5969.
- Siddell, S., Sawicki, D., Meyer, Y., Thiel, V., Sawicki, S., 2001. Identification of the mutations responsible for the phenotype of three MHV RNA-negative ts mutants. *Adv. Exp. Med. Biol.* 494, 453–458.

- Snijder, E.J., Bredenbeek, P.J., Dobbe, J.C., Thiel, V., Ziebuhr, J., Poon, L.L., Guan, Y., Rozanov, M., Spaan, W.J., Gorbalenya, A.E., 2003. Unique and conserved features of genome and proteome of SARS-Coronavirus, an early split-off from the coronavirus group 2 lineage. *J. Mol. Biol.* 331 (5), 991–1004.
- Snijder, E.J., van der Meer, Y., Zevenhoven-Dobbe, J., Onderwater, J.J., van der Meulen, J., Koerten, H.K., Mommaas, A.M., 2006. Ultrastructure and origin of membrane vesicles associated with the severe acute respiratory syndrome coronavirus replication complex. *J. Virol.* 80 (12), 5927–5940.
- Su, D., Lou, Z., Sun, F., Zhai, Y., Yang, H., Zhang, R., Joachimiak, A., Zhang, X.C., Bartlam, M., Rao, Z., 2006. Dodecamer structure of severe acute respiratory syndrome coronavirus nonstructural protein nsp10. *J. Virol.* 80 (16), 7902–7908.
- Sutton, G., Fry, E., Carter, L., Sainsbury, S., Walter, T., Nettleship, J., Berrow, N., Owens, R., Gilbert, R., Davidson, A., Siddell, S., Poon, L.L., Diprose, J., Alderton, D., Walsh, M., Grimes, J.M., Stuart, D.I., 2004. The nsp9 replicase protein of SARS-Coronavirus, structure and functional insights. *Structure* 12 (2), 341–353.
- Tan, J., Kusov, Y., Mutschall, D., Tech, S., Nagarajan, K., Hilgenfeld, R., Schmidt, C.L. The “SARS-unique domain” (SUD) of SARS coronavirus is an oligo(G)-binding protein. *Biochem. Biophys. Res. Commun.*, in press.
- Thiel, V., Ivanov, K.A., Putics, A., Hertzog, T., Schelle, B., Bayer, S., Weissbrich, B., Snijder, E.J., Rabenau, H., Doerr, H.W., Gorbalenya, A.E., Ziebuhr, J., 2003. Mechanisms and enzymes involved in SARS coronavirus genome expression. *J. Gen. Virol.* 84 (Pt 9), 2305–2315.
- Tijms, M.A., van Dinten, L.C., Gorbalenya, A.E., Snijder, E.J., 2001. A zinc finger-containing papain-like protease couples subgenomic mRNA synthesis to genome translation in a positive-stranded RNA virus. *Proc. Natl. Acad. Sci. U.S.A.* 98 (4), 1889–1894.
- Uetz, P., 2002. Two-hybrid arrays. *Curr. Opin. Chem. Biol.* 6 (1), 57–62.
- van der Meer, Y., Snijder, E.J., Dobbe, J.C., Schleich, S., Denison, M.R., Spaan, W.J., Locker, J.K., 1999. Localization of mouse hepatitis virus nonstructural proteins and RNA synthesis indicates a role for late endosomes in viral replication. *J. Virol.* 73 (9), 7641–7657.
- von Brunn, A., Teepe, C., Simpson, J.C., Pepperkok, R., Friedel, C.C., Zimmer, R., Roberts, R., Baric, R., Haas, J., 2007. Analysis of intraviral protein–protein interactions of the SARS Coronavirus ORFome. *PLoS ONE* 2, e459.
- von Grotthuss, M., Wyrwicz, L.S., Rychlewski, L., 2003. mRNA cap-1 methyltransferase in the SARS genome. *Cell* 113 (6), 701–702.
- Walhout, A.J., Vidal, M., 2001. High-throughput yeast two-hybrid assays for large-scale protein interaction mapping. *Methods* 24 (3), 297–306.
- Zhai, Y., Sun, F., Li, X., Pang, H., Xu, X., Bartlam, M., Rao, Z., 2005. Insights into SARS-CoV transcription and replication from the structure of the nsp7–nsp8 hexadecamer. *Nat. Struct. Mol. Biol.* 12 (11), 980–986.
- Ziebuhr, J., Thiel, V., Gorbalenya, A.E., 2001. The autocatalytic release of a putative RNA virus transcription factor from its polyprotein precursor involves two paralogous papain-like proteases that cleave the same peptide bond. *J. Biol. Chem.* 276 (35), 33220–33232.